Title
Actin Cytoskeleton Reorganization by Syk Regulates Fcγ Receptor Responsiveness by Increasing Its Lateral Mobility and Clustering

Authors
Jaumouillé, Valentin
Farkash, Yoav
Jaqaman, Khuloud
et al.

Peer reviewed

HHS Public Access

Actin cytoskeleton reorganization by the tyrosine kinase Syk regulates Fcγ receptor responsiveness by increasing its lateral mobility and clustering

Valentin Jaumouillé[1], **Yoav Farkash**[1], **Khuloud Jaqaman**[2], **Raibatak Das**[3], **Clifford A. Lowell**[4], and **Sergio Grinstein**[1,5]

[1]Program in Cell Biology, Hospital for Sick Children, Toronto, ON, M5G1X8, Canada

[2]Department of Biophysics, University of Texas Southwestern Medical Center, Dallas, TX, 75390-8816, USA

[3]Department of Integrative Biology, University of Colorado Denver, Denver, CO 80204, USA

[4]Department of Laboratory Medicine, University of California, San Francisco, CA, 94143-0100, USA

[5]Keenan Research Centre of the Li Ka Shing Knowledge Institute, St. Michael's Hospital, 209 Victoria St., Toronto, M5C 1N8, Canada

Summary

Clustering of immunoreceptors upon association with multivalent ligands triggers important responses including phagocytosis, secretion of cytokines and production of immunoglobulins. We applied single-molecule detection and tracking methods to study the factors that control the mobility and clustering of phagocytic Fcγ receptors (FcγR). While in resting macrophages the receptors exist as monomers, two distinct populations were discernible based on their mobility: some diffuse by apparent free motion, while others are confined within sub-micron boundaries that reduce the frequency of spontaneous collisions. Src-family and Syk kinases determine the structure of the actin cytoskeleton, which is fenestrated, accounting for the heterogeneous diffusion of the FcγR. Stimulation of these kinases during phagocytosis induces reorganisation of the cytoskeleton both locally and distally in a manner that alters receptor mobility and clustering, generating a feedback loop that facilitates engagement of FcγR at the tip of pseudopods, directing the progression of phagocytosis.

Introduction

Immunoreceptors, such as Fc, B cell and T cell receptors, are responsible for the recognition of antigens, whether by themselves or bound to antibodies or MHC molecules. Signalling by

[*]Corresponding author: Sergio Grinstein, Program in Cell Biology, The Hospital for Sick Children, 555 University Avenue, Toronto, Ontario, Canada M5G 1X8. Tel.: +1 416 813 5727; Fax: +1 416 813 5028; sergio.grinstein@sickkids.ca.

these receptors is essential for innate and adaptive immune responses. Detailed studies of their structure in the free and bound states indicate that immunoreceptors do not undergo significant conformational changes upon ligand binding (Woof and Burton, 2004). Instead, immunoreceptor-mediated signalling is elicited by their clustering. Accordingly, immunoreceptor activation is not triggered by monovalent ligands, requiring multivalent stimuli (Holowka et al., 2007; Jones et al., 1985; Odin et al., 1991).

Immunoreceptors possess in their cytosolic domain a tyrosine-based activation motif (ITAM) that upon receptor clustering becomes phosphorylated by Src family kinases, and possibly also by the spleen tyrosine kinase Syk (Kiefer et al., 1998; Nimmerjahn and Ravetch, 2008). The signalling cascade unleashed by phosphorylation of the ITAM causes a marked reorganization of the actin cytoskeleton, culminating with the formation of an immunological synapse (Xie et al., 2013) or, in the case of Fcγ receptors (FcγR), the phagocytosis of target particles (Flannagan et al., 2012). FcγR have been tacitly assumed to exist as monomers that are evenly distributed on the cell surface and move in Brownian fashion. Upon exposure to particles decorated with multiple IgG molecules –their preferred ligand– FcγR are thought to be progressively recruited ("zipper") around the particle (Griffin et al., 1975) as a result of random lateral diffusion. FcγR clustering and hence activation occur as a consequence of such zippering.

The ability of receptors to rapidly diffuse and cluster is predicated on the assumption that biological membranes behave as fluid bilayers (Singer and Nicolson, 1972). However, a number of recent observations question the general applicability of the Singer-Nicolson fluid mosaic model. Firstly, most proteins studied display lateral mobilities that are 5 to 50 times slower in the plasma membrane of cells than in artificially reconstituted bilayers of comparable lipid composition (Kusumi et al., 2005). Secondly, photobleaching recovery determinations suggested that a subset of plasma membrane proteins are immobile (Jacobson et al., 1976; Schlessinger et al., 1976) and a number of proteins undergo anomalous diffusion, rather than the anticipated free diffusion (Crane and Verkman, 2008; Smith et al., 1999). Thirdly, while the fluid mosaic model predicts that lateral mobility should be only marginally sensitive to the size of the molecule and therefore barely affected by oligomerization (Saffman and Delbrück, 1975), the oligomerization of membrane proteins can reduce their diffusion up to 40-fold (Iino et al., 2001). Finally, plasmalemmal proteins dragged by optical tweezers can rebound to their initial location once they escape the optical trap, suggesting the existence of elastic structures that restrict diffusion within the membrane (Sako and Kusumi, 1995). In view of these observations, the fluid mosaic model has been revised in favour of an alternative model, where the plasmalemma is compartmentalized by molecular "fences". The fence-like structures are thought to be generated by membrane-associated "picket" proteins, anchored to the actin filament network juxtaposed to the bilayer (Kusumi et al., 2005). The density and limited mobility of the transmembrane pickets restrict the diffusion of mobile proteins and lipids in the plane of the membrane.

This reinterpretation of the fluid mosaic model, as well as earlier observations indicating that FcγR heterologously expressed in cell lines are partially mobile (Zhang et al., 1995), prompted us to assess experimentally whether FcγR in fact undergo free diffusion. If

confined by pickets and fences, it is unclear whether FcγR could cluster effectively, particularly during the short window of opportunity presented by the casual contact with particles such as microorganisms, which can be mobile. In addition it was of interest to establish whether the rearrangement of the cytoskeleton that accompanies phagocytosis can itself alter the mobility of the receptors (Jaqaman and Grinstein, 2012; Jaumouillé and Grinstein, 2011). To address these questions we analyzed lateral mobility of FcγR at the single-molecule level. Our results indicate that, contrary to earlier assumptions, FcγR behave heterogeneously, displaying confined and freely mobile subpopulations or states. In addition, engagement of a fraction of the FcγR alters the ability of the unengaged receptors to diffuse, potentially amplifying the response.

Results

Heterogeneous mobility of Fc receptors

We studied the behaviour of FcγRIIA in human monocyte-derived macrophages using antibodies to an exofacial epitope. To prevent clustering induced by the detection system, Fab fragments of a monoclonal antibody (clone IV.3) were prepared and visualized on the dorsal surface of the cells by addition of a secondary anti-mouse Fab fragment conjugated to Cy3 or to biotin. When using biotin-conjugated secondary Fab fragments, detection was accomplished using avidin-coupled quantum dots (Qdots), which are considerably brighter and less susceptible to photobleaching than Cy3. Cross-linking was avoided by adding the Qdots to the cells in the cold to minimize lateral displacement, followed by addition of free biotin to occlude the excess binding sites. Labeling was performed at low density (Figure 1A) to distinguish single FcγRIIA molecules. Individual features were detected and tracked using custom-made algorithms (Jaqaman et al., 2008, 2011).

Moment scaling spectrum (MSS) analysis of single trajectories was used to characterize receptor motion (Ewers et al., 2005; Jaqaman et al., 2008, 2011). As illustrated in Figure 1B–D and Supplementary movie 1, FcγRIIA showed heterogeneous behaviour: 64.4±2.4% of the Cy3-labeled receptors displayed apparent free motion, whereas 27.4±2.3% were confined. Similar results were obtained when FcγRIIA were labeled using Qdots: 64.2±1.8% displayed free motion and 30.8±1.9% were largely confined throughout the acquisition period, which was as long as 30 sec (average acquisition was 7.5 sec; Figure 1C–D). The diffusion of a minor fraction of the FcγRIIA (4.9% when using Qdots, 8.2% with Cy3) appeared as directed by a flow. This small fraction remained unchanged under most conditions and will not be discussed further. The median diffusion coefficient of the free receptors was 0.074 ± 0.004 $\mu m^2 \cdot s^{-1}$ when labelled with Cy3 and 0.071 ± 0.005 $\mu m^2 \cdot s^{-1}$ when measured with Qdots. These observations imply that the larger nano-crystal probe did not perturb receptor behaviour. The diffusion coefficients of the confined receptors were estimated to be 0.032 ± 0.005 $\mu m^2 \cdot s^{-1}$ or 0.026 ± 0.002 $\mu m^2 \cdot s^{-1}$ when labelled with Cy3 or Qdots, respectively. If the cells were fixed with paraformaldehyde prior to analysis a single population of immobile receptors was detected, with a negligible diffusion coefficient (0.002 ± 0.002 $\mu m^2 \cdot s^{-1}$; Figure S1A). These observations suggest that the confined FcγRIIA detected in live cells are not firmly tethered to a fixed structure but instead diffuse within circumscribed areas or "corrals". By analysing the localization of individual confined

receptors over periods of up to 30 sec, we determined that the corrals had a mean area of 0.119±0.015 μm^2 (Figure S1B), larger than lipid rafts or protein complex domains, but in the range of actin-based membrane compartments (Kusumi et al., 2012). FcγRIIA did not follow the linear tracks described for CD36 in the same cells (Jaqaman et al., 2011); 93% of FcγRIIA displayed isotropic behaviour (Figure S1C).

The heterogeneous behaviour of the population raised the question whether some of the FcγRIIA would be more susceptible to collisions, and hence to clustering, that could result in receptor activation. Monte Carlo simulations of receptor diffusion (see Methods) indicated that the collision rate was greatly diminished by receptor confinement and became lower as the corral size was reduced (Figure S1D). The simulations also indicated that receptor collision rate increased as the diffusion coefficient was ramped up (Figure S1E). These results predict that freely diffusing receptors would collide more frequently than confined receptors. Of note, the effect of confinement appeared more limited at higher receptor density (Figure S1F–G). The predicted effect of confinement on receptor diffusion prompted us to measure experimentally the frequency of collision events of Cy3-labelled FcγRIIA (Calebiro et al., 2013; Jaqaman et al., 2011). As anticipated, the collision frequency was 1.73±0.12 fold higher for freely diffusing receptors than for those that were confined (Figure 1E). Jointly, these results indicate that, contrary to earlier assumptions, FcγRIIA behave heterogeneously and are differentially predisposed to collide in the presence of multivalent ligands.

The confinement of FcγRIIA is not due to oligomerization or to association with cholesterol-rich microdomains

Co-existence of receptors in different states of aggregation could account for the presence of subpopulations of FcγRIIA with distinct mobility. Although functional evidence suggests that FcR exist as monomers when not engaged by ligands, the possibility of spontaneous dimerization of FcγRIIA has been invoked (Powell et al., 2006). To determine the state of oligomerization of FcγRIIA in the absence of ligand, macrophages were labelled with increasing concentrations of primary anti-FcγRIIA Fab fragments, followed by a constant saturating concentration of Cy3-conjugated secondary Fab. As previously described, individual Cy3 fluorophores display a defined intensity that enables the quantification of labelled molecules in a complex (Jaqaman et al., 2011). As shown in Figure 1F, while the number of detected features increased as the concentration of primary Fab increased, their modal fluorescence intensity remained constant. This suggests that the detected features represent single receptors. To further explore the state of FcγRIIA oligomerization, we performed photobleaching experiments. If the detected features were composed of two or more labelled receptors, their photobleaching would occur stepwise, revealing the number of fluorophores. Figure 1G illustrates that, upon intense illumination, the number of fluorescent features in the field of view decreased progressively as a result of photobleaching. However, the vast majority of the spots disappeared in one single step, leaving the mean intensity of the remaining features unaltered (Figure 1G–H). Together, these experiments indicate that in the absence of ligands FcγRIIA exist largely as monomers. Thus, heterogeneous oligomerization cannot account for the observed subpopulations with differing mobility.

As an alternative, we contemplated the possibility that the fraction of FcγRIIA that displayed confined motion might reside in cholesterol-enriched lipid microdomains (rafts). Such microdomains can act as diffusional traps for membrane proteins (Douglass and Vale, 2005; Suzuki et al., 2007). Indeed, FcγRIIA is a palmitoylated transmembrane protein that can in principle associate with lipid rafts (Kwiatkowska and Sobota, 2001; Rollet-Labelle et al., 2004). To analyze the contribution of cholesterol-enriched microdomains we treated macrophages with methyl-β-cyclodextrin (MβCD). The effectiveness of this treatment was validated using filipin: exposure to MβCD removed $68.7\pm3.8\%$ of the plasmalemmal cholesterol (Figure 2A–B). Treatment with MβCD reduced the diffusion coefficient of the entire population (Figure 2C), as observed previously for a variety of other membrane proteins (Fujiwara et al., 2002; Murase et al., 2004). Remarkably, cholesterol depletion was accompanied by an *increase* in the proportion of confined FcγRIIA (from $32.8\pm2.7\%$ to $48.7\pm4.1\%$ of total), instead of the hypothesized decrease (Figure 2D). These results imply that receptor confinement is not due to association with cholesterol-rich microdomains, consistent with earlier reports (Kwiatkowska and Sobota, 2001; Rollet-Labelle et al., 2004).

The lateral mobility of FcγRIIA is regulated by the tyrosine kinases Src and Syk

We next speculated that a fraction of the FcγRIIA might associate with other molecules, which could alter receptor mobility. Since interactions of FcγRIIA with effector molecules depend on receptor phosphorylation (Nimmerjahn and Ravetch, 2008), we assessed this possibility using kinase inhibitors. Two types of tyrosine kinases are known to phosphorylate the ITAM of FcγR: Src-family kinases (SFK) and Syk (Ghazizadeh et al., 1994; Kiefer et al., 1998). When active, these kinases undergo autophosphorylation, and the occurrence of this event can be monitored using specific antibodies (anti-pTyr[416] in the case of Src and anti-pTyr[525/526] for Syk). The effectiveness of PP1 (a SFK inhibitor) and of piceatannol (a Syk inhibitor) was verified using such antibodies (Figure 3A–B and S2A). Having demonstrated effective inhibition of SFK, we tested the effect of PP1 on FcγRIIA mobility by single-particle tracking (SPT). Rather than increasing the mobility of the receptors, as would be anticipated by dissolution of preformed complexes, inhibition of SFK activity *increased* the proportion of confined FcγRIIA (from $31.2\pm1.2\%$ to $43.9\pm3.5\%$) and decreased the overall diffusion coefficient (from $0.058\pm0.002\ \mu m^2\cdot s^{-1}$ to $0.038\pm0.005\ \mu m^2\cdot s^{-1}$; Figure 3C–D). Inhibition of Syk had an even more pronounced effect, increasing the proportion of confined FcγRIIA to $62.2\pm4.7\%$ while decreasing the diffusion coefficient to $0.021\pm0.005\ \mu m^2\cdot s^{-1}$ (Figure 3C–D). To minimize the possibility that off-target effects were responsible for the changes caused by piceatannol, we also tested Bay 61-3606, a structurally unrelated Syk inhibitor. Like piceatannol, Bay 61-3606 increased the proportion of confined FcγRIIA (to $43.4\pm2.7\%$) and decreased its diffusion coefficient (to $0.046\pm0.004\ \mu m^2\cdot s^{-1}$; Figure S2B–C). More definitive evidence that the observed effects were in fact attributable to Syk was obtained using macrophages obtained from Syk-deficient mice (Crowley et al., 1997). Because FcγRIIA is not expressed in mice, we measured instead the behavior of FcγRIIB/FcγRIII using a Fab fragment from antibody 2.4G2, which recognizes these receptors. Analysis of FcγRIIB/FcγRIII mobility in mouse macrophages yielded results that were very similar to those obtained for human FcγRIIA. In wild-type cells $61.7\pm3.2\%$ of the receptors underwent free motion, whereas $32.3\pm3.4\%$ were confined (Figure 3E). The diffusion coefficient was $0.052\pm0.006\ \mu m^2\cdot s^{-1}$ (Figure 3F). In *syk*^{−/−}

macrophages however, only 38.2±2.4% of the FcγR underwent free motion, whereas 57.8±2.6% were confined, and the diffusion coefficient dropped to 0.018±0.002 $\mu m^2 \cdot s^{-1}$ (Figure 3E–F). Thus, phosphorylation-dependent association of receptors with effector proteins cannot explain the presence of a confined subpopulation of FcγR. On the other hand, our results revealed an unprecedented role of SFK and Syk in regulating the mobility of FcγRIIA and FcγRIIB.

Syk governs FcγRIIA lateral mobility independently of receptor phosphorylation

Because the inhibition or deletion of the tyrosine kinases had an unexpected effect on FcγR mobility, we investigated whether the altered behaviour was due to changes in the phosphorylation of the receptor itself. To this end we heterologously expressed either wild-type FcγRIIA or a mutant form in which the three tyrosines that are susceptible to phosphorylation were replaced by phenylalanines (termed 3Y-F; Figure 4A). The murine RAW264.7 line (referred to as RAW cells hereafter) was used for transfection, as these macrophages do not express endogenous FcγRIIA, and the receptors were labelled with Qdots. Analysis of FcγRIIA mobility showed that 51.7±1.3% of the wild-type receptors were freely mobile, while 44.1±1.4% were confined (Figure 4B). Thus, the heterogeneous behaviour of FcγRIIA was recapitulated in a heterologous expression system. Moreover, as in the human cells, piceatannol treatment increased the fraction of confined receptors (to 75.4±2%) while lowering the fraction of free FcγRIIA (to 21.8±1.8%; Figure 4B). Interestingly, when expressed in untreated RAW cells the mutant FcγRIIA behaved identically to the wild-type receptor. Of note, piceatannol treatment increased the confinement of the mutant receptor to the same extent as observed for wild-type FcγRIIA (Figure 4B). Similarly, the diffusion coefficients of wild-type and mutant receptors were not significantly different in untreated cells and were comparably depressed by treatment with piceatannol (Figure 4C). Since the 3Y-F mutant cannot be tyrosine phosphorylated, these results demonstrate that Syk exerts its effects on FcγR mobility by a mechanism other than direct receptor phosphorylation.

The actin cytoskeleton governs FcγRIIA mobility

Immunoreceptors, as well as other proteins that associate with the ITAM-containing subunits DAP12 or FcR γ-chain (FcRγ), utilize Syk to transduce signals (Mócsai et al., 2010). One of the downstream effects of these signalling cascades is a local reorganisation of the actin cytoskeleton. In view of the "picket-fence" model of membrane architecture, we considered whether the effects of Syk on FcγRIIA mobility are mediated by remodelling the submembranous actin. To this end we treated macrophages with an actin polymerization inhibitor. We were able to perform SPT using a short (10 min) treatment with a moderate dose (1 μM) of latrunculin B, which caused a partial disruption of the actin cytoskeleton without detaching the cells from the coverslip or grossly altering their morphology. As reported for other immunoreceptors (Andrews et al., 2008; Treanor et al., 2010), this treatment increased the diffusion coefficient of FcγRIIA (to 0.089±0.004 $\mu m^2 \cdot s^{-1}$; Figure 5A). Interestingly, this increased diffusion coefficient is accompanied by a 46% reduction in the proportion of confined receptors (to 18.8±1.3%), with a commensurate increase in the freely diffusing fraction (to 74.6±1.5%; Figure 5B).

Because a more thorough disassembly of the actin cytoskeleton leads to changes in cell morphology, precluding accurate tracking of single particles, we extended our analysis of the role of the cytoskeleton in FcγRIIA mobility using an alternative method, namely Fluorescence Recovery After Photobleaching (FRAP). For these experiments RAW cells were transfected with GFP-tagged FcγRIIA and receptor mobility in otherwise untreated membranes was compared with that in membrane blebs devoid of actin (Booth et al., 2002). These were generated by treating macrophages with jasplakinolide. Stabilization of the cortical actin by jasplakinolide causes a myosin II-dependent contraction of the cytoskeleton, with concomitant extrusion of actin-depleted membrane blebs (Flannagan et al., 2010). The contraction of the cortical actin band was verified by co-transfecting the cells with LifeAct, a probe that binds specifically to F-actin (Riedl et al., 2008). Figure 5C shows not only that F-actin underwent contraction following addition of jasplakinolide, but also that the membrane blebs lacked detectable F-actin, yet contained GFP-tagged FcγRIIA. In the absence of jasplakinolide, the diffusion coefficient of FcγRIIA-GFP estimated by FRAP was $0.035 \pm 0.02 \ \mu m^2 \cdot s^{-1}$ (Figure 5D), consistent with data we obtained by SPT in the same cell line. By contrast, FcγRIIA-GFP diffusion was markedly faster within membrane blebs ($D = 0.119 \pm 0.103 \ \mu m^2 \cdot s^{-1}$; Figure 5D). Combined with the SPT determinations in latrunculin-treated cells, these results demonstrate that the cortical actin is a major determinant of the lateral mobility of FcγRIIA, restricting receptor diffusion.

Syk regulates FcγRIIA mobility by organizing the cortical actin meshwork

Syk is intimately involved in the reorganization of actin during phagocytosis. It is therefore conceivable that tonic Syk activity may contribute also to the establishment and/or maintenance of the basal cytoskeletal structure of unstimulated macrophages; such a contribution could account for the effects of Syk on FcγRIIA mobility described above. This was investigated by staining F-actin with rhodamine-phalloidin and comparing the appearance of the cytoskeleton in the presence and absence of Syk inhibitors, using confocal microscopy. As expected, untreated macrophages displayed a band of cortical actin lining the dorsal membrane, and a large number of intensely stained ventral podosomes (Figure 6A, S2A and S3A). Strikingly, upon treatment with piceatannol the podosomes became virtually undetectable and, instead, F-actin staining increased markedly under the dorsal membrane. As a result, the ratio of dorsal to ventral actin increased from 0.67 ± 0.07 in controls to 1.77 ± 0.2 after inhibition of Syk (Figure 6B). Despite this pronounced redistribution, the total amount of cellular F-actin was not significantly changed by piceatannol (Figure 6C).

As Syk is known to regulate the activity of several GEFs for Rac1 and RhoA, which in turn control actin polymerization, we determined the activity of these GTPases in macrophages using the PBD domain of PAK1 or rhotekin, respectively (see Methods). In piceatannol-treated cells Rac1 activity decreased to $58.4 \pm 4\%$, whereas RhoA activity increased to $151 \pm 1.9\%$ of the control level (Figure S3B). These changes were associated with a decrease in the rate of actin polymerization; piceatannol reduced the rate of monomeric actin association with the barbed ends of filaments to $71.7 \pm 8.8\%$ of the control (Figure S3C).

While regulation of Rho-family GTPase activity by Syk can account for the cytoskeletal alterations, it does not clarify how the associated changes in F-actin distribution restrict the mobility of FcγRIIA. To gain further insight we analyzed the ultrastructure of the cortical actin that lines the dorsal membrane, the surface where receptor mobility was assessed. This was accomplished by visualizing the cytoskeletal meshwork in cells that were demembranated by non-ionic detergent in an actin filament-stabilizing buffer (Svitkina, 2007), prior to fixation and preparation for high-resolution scanning electron microscopy using field emission. As illustrated in Figure 6D, in untreated cells the cytoskeleton was very heterogeneous, consisting of patches of dense networks of microfilaments, separated by relatively open areas devoid of filamentous material (Figure 6D). Following incubation with the Syk inhibitor the patches of filamentous meshwork were larger and denser, separated by much smaller open areas (Figure 6D). Thus, the ultrastructure of the dorsal cortical actin network correlated with the results obtained with phalloidin and can explain the SPT results: receptors located in the open areas presumably diffuse freely in the plane of the membrane, while those in areas lined by an actin meshwork undergo confinement. The increase in the number and density of the latter accounts for the confining effects of piceatannol and of genetic ablation of Syk.

A corollary of this hypothesis is that inhibition of Syk should have no effect on receptors localized in areas devoid of the actin cytoskeleton. The validity of this corollary was tested by FRAP measurements in jasplakinolide-induced blebs, which lack detectable actin (see Figure 5C). As predicted, the rapid diffusion of GFP-tagged FcγRIIA in blebs formed by jasplakinolide-treated RAW cells was unaffected by addition of piceatannol: the diffusion coefficient was $0.108\pm0.088~\mu m^2 \cdot s^{-1}$ in the presence of the inhibitor, compared to $0.119\pm0.103~\mu m^2 \cdot s^{-1}$ in its absence. By contrast, piceatannol markedly reduced the diffusion rate of receptors in the membrane of cells not treated with jasplakinolide, decreasing the diffusion coefficient from $0.035\pm0.02~\mu m^2 \cdot s^{-1}$ to $0.017\pm0.008~\mu m^2 \cdot s^{-1}$ (Figure 5D). These results confirm that the effects of piceatannol are specific, attributable to alterations in cytoskeletal structure.

Syk regulates FcγR lateral mobility within the phagocytic cup

The preceding results indicate that: a) FcγR mobility is constrained by an inhomogeneous layer of cortical actin and b) Syk influences the structure of the cortical cytoskeleton in resting cells. Because the cytoskeleton is acutely remodelled during the early stages of phagocytosis, and because Syk is stimulated early in the process, it is likely that the initial engagement of FcγR modifies the ability of the remaining, unengaged receptors to move, thereby modulating their responsiveness. Evaluating the occurrence and magnitude of this purported feedback mechanism requires an understanding of the effects of Syk on cytoskeletal structure. Our results above indicate that, in resting macrophages, Syk activity is associated with *reduced* dorsal actin. This observation appears paradoxical, because Syk is essential for the engulfment of IgG-coated particles (Crowley et al., 1997; Kiefer et al., 1998), a process that entails net actin polymerization at the phagocytic cup. However, whether Syk is required for polymerization remains unclear, because –at least in a few instances– actin remodelling at the phagocytic cup has been reported to persist when the kinase was inhibited or genetically ablated (Cougoule et al., 2006; Crowley et al., 1997). As

illustrated in Figure 7A and Movie S2 top, we were able to recapitulate these observations: in RAW macrophages expressing LifeAct-GFP, F-actin clearly accumulated at the base of forming phagosomes, despite inhibition of Syk by piceatannol. Note, however, that inhibition of Syk arrested progression of the pseudopods around the target particle, precluding engulfment. The stage at which Syk exerts its effects was more clearly visualized using an alternative experimental model. RAW cells stably expressing actin-GFP were suspended and allowed to settle onto IgG-coated coverslips, thereby initiating frustrated phagocytosis (Figure 7B). The use of this model ensures that the surface where receptor engagement occurs remains in the focal plane throughout the phagocytic event. Untreated macrophages spread on the IgG-coated surface, assembling vast amounts of actin at sites of contact. As polymerization progresses outwardly, three distinct regions can be identified: an actin-poor outer lamellipodium at the advancing edge, an actin-rich ring, and an area of actin clearance at the center of the frustrated phagosome (Figure 7C top, Movie S2 bottom); this region is equivalent to the base of the phagocytic cup, where a comparable clearance zone develops as the pseudopods advance (see Figure 7A). When cells were pretreated with piceatannol the early phases of actin polymerization, though attenuated, were still observed at sites of contact. However, these failed to advance and the extension of the lamellipodium and the development of the clearance zone were impaired (Figure 7C, Supplementary movie 3). Thus, Syk activity seems to be required for the disassembly of actin that enables pseudopod progression. This contribution of Syk to actin depolymerisation is akin to the effect of the kinase in resting cells.

Having established the pattern of actin polymerization during frustrated phagocytosis, we took advantage of this model to measure the mobility of unengaged FcγR in regions of varying F-actin density. FcγRIIB and FcγRIII were labeled at low density on the surface of suspended, actin-GFP expressing macrophages. The labeled cells were then allowed to settle onto IgG-coated coverslips, initiating phagocytosis. Importantly, the Fab fragment used to label the FcγR interacts with the Fc-binding domain of the receptors, preventing engagement by ligands. Thus, the behaviour of free receptors could be monitored while others were being engaged by the IgG on the coverslip. By imaging GFP-actin we were able to select a stage of phagocytosis when the phagocytic cup had developed (Figure 7D) and used this window of time to record FcγR mobility. The MSS analysis showed that the majority of the unengaged receptors were freely mobile at the fringe of the cup, where actin was less dense (66.9±4.9% free motion, 23±3.9% confined). By contrast, the majority (61.9±7.2%) of the receptors present in the ring formed by densely polymerized actin (selected for analysis using a thresholding algorithm) were confined (Figure 7E).

As Syk inhibition did not prevent the initial burst of actin polymerization but rather impaired progression of the pseudopods and actin clearance from the middle of the forming phagosome, we were also able to measure receptor mobility at nascent cups in the presence of piceatannol. When mobility was measured at sites of frustrated phagocytosis in the presence of the inhibitor, the fraction of confined receptors reached 76.5±10.9%, whereas only 15.1±8.5% of the FcγR underwent free motion (Figure 7F). These observations demonstrate that activation of actin polymerization during phagocytosis restricts the mobility of unengaged FcγR, whereas activation of Syk restores their mobility by inducing actin clearance.

Discussion

Our observations enabled us to reach three main conclusions: a) at least two subpopulations or states of FcγR exist in quiescent cells; b) Syk is an important determinant of actin structure and receptor mobility in unstimulated macrophages, and c) the Syk-mediated restructuring of the cytoskeleton initiated by FcγR stimulation exerts a feedback effect on receptor mobility and hence on receptor responsiveness during phagocytosis. The implications of these conclusions are discussed in turn.

FcγR undergo transitions between free and confined modes of diffusion

Our experiments were designed to test the validity of several of the premises that underlie the zippering model of phagocytosis. While we confirmed that in resting cells FcγRIIA exist almost exclusively as monomers, we identified two subpopulations (or states) with distinct mobility properties. The receptors undergo transitions between fast and slow diffusion states, which could be resolved using a two-state hidden Markov model analysis (Das et al., 2009). Because the rate of transition from the slow to the fast state is greater than the rate of the opposite transition (Supplemental Figure 7), the receptors appear to diffuse freely for a majority of the time ($\approx$70%) in untreated cells (Figure 3). It is noteworthy that a relatively slow acquisition rate (33 Hz) was employed in our studies. Therefore the transitions between slow and fast states reported here should be distinguished from the hop-diffusion mechanism described earlier (Kusumi et al., 2012). Rather than reflecting the escape of proteins via openings in persistent corrals, the slower transitions reported here are probably due to larger scale alterations in the structure of the actin network.

It is noteworthy that when Syk is inhibited, the rate constant of transition from the fast to the slow state increases, while the reverse rate constant decreases (Figure S4). Thus, Syk activity appears to prevent receptors from entering confinement regions. But once trapped in a confinement region, receptors have roughly the same probability of escape independent of Syk activity. The net result of Syk inhibition is a greater propensity for the receptors to be transiently confined.

A new role of Syk in cytoskeleton organization

While there was abundant evidence for a role of Syk in actin reorganization upon immunoreceptor stimulation, our study revealed that the kinase is partially active in resting macrophages and plays a major role in the general organization of the actin cytoskeleton (Figs. 3 and 6). What causes Syk activity in macrophages at rest? Activation of the kinase is typically triggered by association with phosphorylated ITAM (Mócsai et al., 2010), which are in turn generated by receptor stimulation. Since FcR are the most abundant ITAM-bearing receptors in macrophages, one can envision that, even in the absence of ligand, FcR occasionally coalesce randomly, resulting in stimulation of Syk activity. While not described for FcR, such stimulation by random collisions has been documented for B cell receptors (Monroe, 2006). Of note, altering B cell receptor confinement by disrupting the actin cytoskeleton was found to enhance the tonic signalling, likely due to increased receptor mobility and spontaneous coalescence (Treanor et al., 2010). Our analysis of receptor trajectories in resting cells showed that FcγRIIA can randomly merge and split, consistent

with the hypothesis of tonic signalling (Figure 1E). However, our studies of the oligomerization state FcγRIIA demonstrated that, if random events occur, only an extremely limited number of receptors would be clustered at any given time (Figure 1F–G). Therefore, it is likely that other mechanisms contribute to the tonic stimulation of Syk.

Several membrane receptors associate with the ITAM-bearing subunits DAP12 or FcRγ, potentially leading to Syk activation (Mócsai et al., 2010). In myeloid cells, the best-characterized example is the adhesion-dependent stimulation of Syk, which requires engagement of integrins that interact with ITAM-containing adaptors (Mócsai et al., 2002). Our observations that Syk inhibition led to podosome disassembly (Figure 6), and that the majority of active Syk (visualized using anti-pSyk antibody; Figure S2A) co-localized with podosomes, are suggestive of integrin-mediated activation of Syk in resting macrophages. Accordingly, inhibition of integrin-mediated adhesion by EDTA greatly reduced Syk activation (Figure S2A). However, the list of receptors that can interact with DAP12 or FcRγ is relatively large (Fodor et al., 2006). Hence, basal Syk activity in "unstimulated" macrophages likely results from several different signalling pathways.

It is important to note that, despite localizing almost exclusively to the ventral surface of the cell, where integrin-mediated adherence takes place, active Syk affects the state of actin on both the ventral and dorsal aspects of the membrane. Thus, Syk exerts control of local as well as distal actin polymerization. How are these effects mediated? The master regulators of actin organization are molecular switches of the Rho GTPase family (Heasman and Ridley, 2008). Syk is known to regulate the activity of Rho-family GEFs, including Vav isoforms that activate Rac and RhoA (Deckert et al., 1996). We find that in adherent macrophages piceatannol inhibits Rac1 (accounting for the dissolution of podosomes), but activates RhoA (Figure S3B). This effect is correlated with increased cortical actin density at the dorsal surface, which was recapitulated by the over-expression of constitutively active RhoA (not shown).

The cortical actin of macrophages has a fenestrated appearance, when visualized by scanning electron microscopy. This peculiar cytoskeletal structure accounts for the co-existence of freely mobile receptors, likely present in fenestrations, and confined receptors presumably found in actin-rich patches. By modulating the cytoskeletal structure, the tonic activity of Syk influences the ratio of freely mobile and confined receptors and their diffusion coefficient. Our results imply that such tonic activity increases the overall mobility of the FcR, improving their likelihood of clustering when confronted with a multivalent ligand.

Functional consequences of actin reorganization by Syk during phagocytosis: the zipper model revisited

Syk not only influences the cytoskeletal structure of resting macrophages, but causes striking actin rearrangements when it undergoes stimulation during FcR engagement. Inevitably, this will impact the mobility and responsiveness of those receptors not yet immobilized by interaction with particle-bound IgG, generating a feedback effect that was previously unappreciated. Our observations of FcγR mobility during phagocytosis show that receptors are more mobile at the periphery of the cup (visualized as a lamellipodium during

frustrated phagocytosis) than at the level of the dense actin ring (Figure 7D). Since receptor coalescence requires their diffusional displacement, this differential mobility favours clustering of unengaged receptors at the edge of the advancing lamellipodium/pseudopod, whereas further receptor recruitment is prevented in areas where signalling has already reached a sufficient level to induce intense actin polymerization. This combination of positive feedback at the leading edge and negative feedback in actin-enriched areas is ideally suited to foster receptor engagement and effective progress of the pseudopod tip, while limiting excessive and unnecessary signalling in activated regions.

These observations have clear physiological implications: the degree of integrin engagement during leukocyte chemotaxis to sites of infection will influence the preparedness of the receptors to engage the IgG-coated prey. Secondly, in the course of phagocytosis the activation of Syk and the attendant cytoskeletal remodelling direct receptor mobility in a manner that optimizes target engulfment while preventing unnecessary and possibly counterproductive stimulation in areas where the cytoskeleton has been sufficiently rearranged.

Experimental procedures

Reagents

Reagent details are provided in the supplemental information.

Macrophage isolation and culture

Human blood samples from healthy volunteers were collected with heparin. Peripheral blood mononuclear cells were isolated by density-gradient centrifugation using Ficoll-Paque Plus (Amersham). Cells were resuspended (10^7 cells/mL) in RPMI-1640 with L-glutamine containing 10% heat-inactivated fetal bovine serum (FBS; Wisent) and seeded onto 18 mm glass coverslips (Fisher Scientific) at 5 x 10^5 cells/coverslip. After 1 h at 37°C, non-adherent cells were removed by multiple washes. Adherent cells were incubated in RPMI-1640 with 10% FCS, 1 ng/mL human M-CSF and 100 U/mL penicillin, 100 μg/mL streptomycin and 10 μg/mL polymyxin B (Invitrogen) for 7–14 days.

To prepare bone marrow derived macrophages, femurs and tibias were dissected form euthanized mice. The marrow was extracted by perfusion of DMEM with a 21-gauge needle to produce a single-cell suspension, which was plated in DMEM with 10% FBS, 1 ng/mL murine M-CSF and 100 U/mL penicillin, 100 μg/mL streptomycin and 10 μg/mL polymyxin B (Invitrogen). After removal of non-adherent cells, macrophages were cultured for 7 days to allow complete maturation.

Receptor labelling and single-particle tracking (SPT)

Cells were blocked in HEPES-buffered RPMI-1640 (HPMI) with 5% donkey serum for 5 min and incubated for 10 min with IV.3 Fab fragments (specific to human FcγRIIA), or anti mouse FcγR Fab fragments (Flannagan et al., 2010), diluted in blocking medium. Next, cells were incubated with Cy3-conjugated donkey anti-mouse Fab fragments, or biotinylated Fab fragments, at a 1:1000 dilution for 10 min. In the latter case, cells were then washed in

HBSS and incubated with streptavidin-conjugated Qdot 655 for 4 min. Finally, cells were washed 3 times in HPMI containing 0.2 μg/mL biotin to block unengaged streptavidin.

Images were acquired on a Zeiss Axiovert 200M microscope, equipped with a 100x NA 1.45 oil objective, a custom 2.4x magnification lens and a back-thinned EM-CCD camera (C9100-13, Hamamatsu). Acquisitions were performed at 33 Hz with Volocity software (Perkin-Elmer). Single particles were detected and tracked as described (Jaqaman et al., 2008, 2011). Motion types and diffusion coefficients were determined using a Moment Scaling Spectrum (MSS) analysis (Ewers et al., 2005; Ferrari et al., 2001; Jaqaman et al., 2011). The confinement dimension was derived by eigenvalue decomposition of the variance-covariance matrix of particle positions (Jaqaman et al., 2011).

Fluorescence recovery after photobleaching

RAW macrophages transfected with FcγRIIA-GFP were imaged using a Nikon A1R confocal microscope running Nikon Elements 4.1. Simultaneous photobleaching/imaging was performed using resonance mode (512 x 512, 30 fps) with a 60x/1.4 CFI Apo Lambda S oil objective and 401/488 nm laser lines, respectively. To determine the rate of recovery, fluorescence intensity of the bleached and an unbleached area were measured in the same cell. The intensity of the bleached area was normalized to that of the corresponding unbleached area to correct for general photobleaching due to sampling. Data were fitted to a simple diffusion, zero-flow model using the formula:

$$F_{(t)} = (F_{(t=0)} + F_{(t=\infty)}\,(t/t_{1/2}))/(1 + (t/t_{1/2}))$$

where the fluorescence intensity (F) at a given time (t) is related to the maximal fluorescence ($F(t=\infty)$) and the half-time of maximal recovery ($t_{1/2}$) (Yguerabide et al., 1982). Recovery curves were fitted using this equation, with Prism 4 (GraphPad Software). Diffusion coefficients were calculate using the following formula:

$$D = (\omega^2/4t_{1/2})\,\gamma_D$$

where ω is the width of the bleached area and γ_D is a constant equal to 0.88 (Axelrod et al., 1976).

Scanning electron microscopy

Imaging of the cortical cytoskeleton by scanning electron microscopy was performed as described previously (Svitkina, 2007). Briefly, cell membranes were extracted for 5 min at room temperature by 1% Triton X-100 and 4% polyethylene glycol (MW 40,000) in PEM buffer (100 mM PIPES, pH 6.9; 1 mM MgCl₂; 1 mM EGTA), supplemented with 10 μg/mL taxol and 10 μM phalloidin. Cells were then washed and immediately fixed with 2% glutaraldehyde in PEM buffer for 20 min. After removing the fixative, cells were incubated with 0.1% tannic acid for 20 min. Cells were rinsed 3 times in distilled water, then incubated in 0.2% uranyl acetate for 20 min. Samples were dehydrated in graded ethanol solutions and

critical point-dried in CO_2. Finally, samples were coated with platinum and carbon. Images were acquired on a Hitachi field emission scanning electron microscope.

Phagocytosis and frustrated phagocytosis assays

Fc-mediated phagocytosis of particles was performed using 5 μm polystyrene beads with 2% DVB (Bang's Laboratories) coated with human IgG at 1 mg/mL for 1 hour at room temperature. Beads were washed 3 times and added to the cells in HPMI at 37°C. Phagocytosis was imaged using a Quorum spinning-disc confocal microscope. For frustrated phagocytosis, glass coverslips were coated with 1% BSA in PBS for 1 hour at room temperature. Coverslips were washed 3 times and then incubated with a mouse monoclonal anti-BSA antibody (Serotech) at 1:50 for 1 hour. Coverslips were washed 3 times and placed in HPMI at 37°C. Suspended RAW macrophages stably expressing actin-GFP were added to the medium and imaged. For SPT, RAW macrophages were labelled with anti mouse FcγR Fab fragments as described above, prior to their suspension.

Image processing, quantification and statistics

Images were acquired using Volocity 4 (Perkin-Elmer), exported as Tiff and processed with MatLab (MathWorks) for SPT, or analysed and quantified using ImageJ 1.46 (NIH) for all the other experiments. Statistical comparison of the data was performed by the nonparametric Mann-Whitney test, with a two-tailed P value, using Prism 4 (GraphPad Software). For each measurement, mean and standard error of the mean (presented as error bars) were calculated from at least three independent experiments.

Supplementary Material

Refer to Web version on PubMed Central for supplementary material.

Acknowledgments

References

Andrews NL, Lidke KA, Pfeiffer JR, Burns AR, Wilson BS, Oliver JM, Lidke DS. Actin restricts FcepsilonRI diffusion and facilitates antigen-induced receptor immobilization. Nat Cell Biol. 2008; 10:955–963. [PubMed: 18641640]

Axelrod D, Koppel DE, Schlessinger J, Elson E, Webb WW. Mobility measurement by analysis of fluorescence photobleaching recovery kinetics. Biophys J. 1976; 16:1055–1069. [PubMed: 786399]

Booth JW, Kim MK, Jankowski A, Schreiber AD, Grinstein S. Contrasting requirements for ubiquitylation during Fc receptor-mediated endocytosis and phagocytosis. EMBO J. 2002; 21:251–258. [PubMed: 11823418]

Calebiro D, Rieken F, Wagner J, Sungkaworn T, Zabel U, Borzi A, Cocucci E, Zürn A, Lohse MJ. Single-molecule analysis of fluorescently labeled G-protein-coupled receptors reveals complexes with distinct dynamics and organization. Proc Natl Acad Sci USA. 2013; 110:743–748. [PubMed: 23267088]

Cougoule C, Hoshino S, Dart A, Lim J, Caron E. Dissociation of recruitment and activation of the small G-protein Rac during Fcgamma receptor-mediated phagocytosis. J Biol Chem. 2006; 281:8756–8764. [PubMed: 16434390]

Crane JM, Verkman AS. Long-range nonanomalous diffusion of quantum dot-labeled aquaporin-1 water channels in the cell plasma membrane. Biophys J. 2008; 94:702–713. [PubMed: 17890385]

Crowley MT, Costello PS, Fitzer-Attas CJ, Turner M, Meng F, Lowell C, Tybulewicz VL, DeFranco AL. A critical role for Syk in signal transduction and phagocytosis mediated by Fcgamma receptors on macrophages. J Exp Med. 1997; 186:1027–1039. [PubMed: 9314552]

Das R, Cairo CW, Coombs D. A hidden Markov model for single particle tracks quantifies dynamic interactions between LFA-1 and the actin cytoskeleton. PLoS Comput Biol. 2009; 5:e1000556. [PubMed: 19893741]

Deckert M, Tartare-Deckert S, Couture C, Mustelin T, Altman A. Functional and physical interactions of Syk family kinases with the Vav proto-oncogene product. Immunity. 1996; 5:591–604. [PubMed: 8986718]

Douglass AD, Vale RD. Single-molecule microscopy reveals plasma membrane microdomains created by protein-protein networks that exclude or trap signaling molecules in T cells. Cell. 2005; 121:937–950. [PubMed: 15960980]

Ewers H, Smith AE, Sbalzarini IF, Lilie H, Koumoutsakos P, Helenius A. Single-particle tracking of murine polyoma virus-like particles on live cells and artificial membranes. Proc Natl Acad Sci USA. 2005; 102:15110–15115. [PubMed: 16219700]

Ferrari R, Manfroi AJ, Young WR. Strongly and weakly self-similar diffusion. Physica D. 2001; 154:111–137.

Flannagan RS, Harrison RE, Yip CM, Jaqaman K, Grinstein S. Dynamic macrophage "probing" is required for the efficient capture of phagocytic targets. J Cell Biol. 2010; 191:1205–1218. [PubMed: 21135140]

Flannagan RS, Jaumouillé V, Grinstein S. The cell biology of phagocytosis. Annu Rev Pathol. 2012; 7:61–98. [PubMed: 21910624]

Fodor S, Jakus Z, Mócsai A. ITAM-based signaling beyond the adaptive immune response. Immunol Lett. 2006; 104:29–37. [PubMed: 16332394]

Fujiwara T, Ritchie K, Murakoshi H, Jacobson K, Kusumi A. Phospholipids undergo hop diffusion in compartmentalized cell membrane. J Cell Biol. 2002; 157:1071–1081. [PubMed: 12058021]

Ghazizadeh S, Bolen JB, Fleit HB. Physical and functional association of Src-related protein tyrosine kinases with Fc gamma RII in monocytic THP-1 cells. J Biol Chem. 1994; 269:8878–8884. [PubMed: 8132624]

Griffin FM, Griffin JA, Leider JE, Silverstein SC. Studies on the mechanism of phagocytosis. I. Requirements for circumferential attachment of particle-bound ligands to specific receptors on the macrophage plasma mambrane. J Exp Med. 1975; 142:1263–1282. [PubMed: 1194852]

Heasman SJ, Ridley AJ. Mammalian Rho GTPases: new insights into their functions from in vivo studies. Nat Rev Mol Cell Biol. 2008; 9:690–701. [PubMed: 18719708]

Holowka D, Sil D, Torigoe C, Baird B. Insights into immunoglobulin E receptor signaling from structurally defined ligands. Immunol Rev. 2007; 217:269–279. [PubMed: 17498065]

Iino R, Koyama I, Kusumi A. Single molecule imaging of green fluorescent proteins in living cells: E-cadherin forms oligomers on the free cell surface. Biophys J. 2001; 80:2667–2677. [PubMed: 11371443]

Jacobson K, Derzko Z, Wu ES, Hou Y, Poste G. Measurement of the lateral mobility of cell surface components in single, living cells by fluorescence recovery after photobleaching. J Supramol Struct. 1976; 5:565(417), 576(428). [PubMed: 800621]

Jaqaman K, Grinstein S. Regulation from within: the cytoskeleton in transmembrane signaling. Trends Cell Biol. 2012; 22:515–526. [PubMed: 22917551]

Jaqaman K, Loerke D, Mettlen M, Kuwata H, Grinstein S, Schmid SL, Danuser G. Robust single-particle tracking in live-cell time-lapse sequences. Nat Methods. 2008; 5:695–702. [PubMed: 18641657]

Jaqaman K, Kuwata H, Touret N, Collins R, Trimble WS, Danuser G, Grinstein S. Cytoskeletal control of CD36 diffusion promotes its receptor and signaling function. Cell. 2011; 146:593–606. [PubMed: 21854984]

Jaumouillé V, Grinstein S. Receptor mobility, the cytoskeleton, and particle binding during phagocytosis. Curr Opin Cell Biol. 2011; 23:22–29. [PubMed: 21074980]

Jones DH, Nusbacher J, Anderson CL. Fc receptor-mediated binding and endocytosis by human mononuclear phagocytes: monomeric IgG is not endocytosed by U937 cells and monocytes. J Cell Biol. 1985; 100:558–564. [PubMed: 3968180]

Kiefer F, Brumell J, Al-Alawi N, Latour S, Cheng A, Veillette A, Grinstein S, Pawson T. The Syk protein tyrosine kinase is essential for Fcgamma receptor signaling in macrophages and neutrophils. Mol Cell Biol. 1998; 18:4209–4220. [PubMed: 9632805]

Kusumi A, Nakada C, Ritchie K, Murase K, Suzuki K, Murakoshi H, Kasai RS, Kondo J, Fujiwara T. Paradigm shift of the plasma membrane concept from the two-dimensional continuum fluid to the partitioned fluid: high-speed single-molecule tracking of membrane molecules. Annu Rev Biophys Biomol Struct. 2005; 34:351–378. [PubMed: 15869394]

Kusumi A, Fujiwara TK, Chadda R, Xie M, Tsunoyama TA, Kalay Z, Kasai RS, Suzuki KGN. Dynamic organizing principles of the plasma membrane that regulate signal transduction: commemorating the fortieth anniversary of Singer and Nicolson's fluid-mosaic model. Annu Rev Cell Dev Biol. 2012; 28:215–250. [PubMed: 22905956]

Kwiatkowska K, Sobota A. The clustered Fcgamma receptor II is recruited to Lyn-containing membrane domains and undergoes phosphorylation in a cholesterol-dependent manner. Eur J Immunol. 2001; 31:989–998. [PubMed: 11298323]

Mócsai A, Zhou M, Meng F, Tybulewicz VL, Lowell CA. Syk is required for integrin signaling in neutrophils. Immunity. 2002; 16:547–558. [PubMed: 11970878]

Mócsai A, Ruland J, Tybulewicz VLJ. The SYK tyrosine kinase: a crucial player in diverse biological functions. Nat Rev Immunol. 2010; 10:387–402. [PubMed: 20467426]

Monroe JG. ITAM-mediated tonic signalling through pre-BCR and BCR complexes. Nat Rev Immunol. 2006; 6:283–294. [PubMed: 16557260]

Murase K, Fujiwara T, Umemura Y, Suzuki K, Iino R, Yamashita H, Saito M, Murakoshi H, Ritchie K, Kusumi A. Ultrafine membrane compartments for molecular diffusion as revealed by single molecule techniques. Biophys J. 2004; 86:4075–4093. [PubMed: 15189902]

Nimmerjahn F, Ravetch JV. Fcgamma receptors as regulators of immune responses. Nat Rev Immunol. 2008; 8:34–47. [PubMed: 18064051]

Odin JA, Edberg JC, Painter CJ, Kimberly RP, Unkeless JC. Regulation of phagocytosis and [Ca2+]i flux by distinct regions of an Fc receptor. Science. 1991; 254:1785–1788. [PubMed: 1837175]

Powell MS, Barnes NC, Bradford TM, Musgrave IF, Wines BD, Cambier JC, Hogarth PM. Alteration of the Fc gamma RIIa dimer interface affects receptor signaling but not ligand binding. J Immunol. 2006; 176:7489–7494. [PubMed: 16751395]

Riedl J, Crevenna AH, Kessenbrock K, Yu JH, Neukirchen D, Bista M, Bradke F, Jenne D, Holak TA, Werb Z, et al. Lifeact: a versatile marker to visualize F-actin. Nat Methods. 2008; 5:605–607. [PubMed: 18536722]

Rollet-Labelle E, Marois S, Barbeau K, Malawista SE, Naccache PH. Recruitment of the cross-linked opsonic receptor CD32A (FcgammaRIIA) to high-density detergent-resistant membrane domains in human neutrophils. Biochem J. 2004; 381:919–928. [PubMed: 15130090]

Saffman PG, Delbrück M. Brownian motion in biological membranes. Proc Natl Acad Sci USA. 1975; 72:3111–3113. [PubMed: 1059096]

Sako Y, Kusumi A. Barriers for lateral diffusion of transferrin receptor in the plasma membrane as characterized by receptor dragging by laser tweezers: fence versus tether. J Cell Biol. 1995; 129:1559–1574. [PubMed: 7790354]

Schlessinger J, Webb WW, Elson EL, Metzger H. Lateral motion and valence of Fc receptors on rat peritoneal mast cells. Nature. 1976; 264:550–552. [PubMed: 1004593]

Singer SJ, Nicolson GL. The fluid mosaic model of the structure of cell membranes. Science. 1972; 175:720–731. [PubMed: 4333397]

Smith PR, Morrison IE, Wilson KM, Fernández N, Cherry RJ. Anomalous diffusion of major histocompatibility complex class I molecules on HeLa cells determined by single particle tracking. Biophys J. 1999; 76:3331–3344. [PubMed: 10354459]

Suzuki KG, Fujiwara TK, Sanematsu F, Iino R, Edidin M, Kusumi A. GPI-anchored receptor clusters transiently recruit Lyn and G alpha for temporary cluster immobilization and Lyn activation: single-molecule tracking study 1. J Cell Biol. 2007; 177:717–730. [PubMed: 17517964]

Svitkina T. Electron microscopic analysis of the leading edge in migrating cells. Methods Cell Biol. 2007; 79:295–319. [PubMed: 17327162]

Treanor B, Depoil D, Gonzalez-Granja A, Barral P, Weber M, Dushek O, Bruckbauer A, Batista FD. The membrane skeleton controls diffusion dynamics and signaling through the B cell receptor. Immunity. 2010; 32:187–199. [PubMed: 20171124]

Woof JM, Burton DR. Human antibody-Fc receptor interactions illuminated by crystal structures. Nat Rev Immunol. 2004; 4:89–99. [PubMed: 15040582]

Xie J, Tato CM, Davis MM. How the immune system talks to itself: the varied role of synapses. Immunol Rev. 2013; 251:65–79. [PubMed: 23278741]

Yguerabide J, Schmidt JA, Yguerabide EE. Lateral mobility in membranes as detected by fluorescence recovery after photobleaching. Biophys J. 1982; 40:69–75. [PubMed: 7139035]

Zhang F, Yang B, Odin JA, Shen Z, Lin CT, Unkeless JC, Jacobson K. Lateral mobility of Fc gamma RIIa is reduced by protein kinase C activation. FEBS Lett. 1995; 376:77–80. [PubMed: 8521972]

Highlights

- Variable FcγR motion types determine their spontaneous collision frequency.

- Tonic Src-family and Syk kinase activity regulates cortical actin architecture.

- Src-family and Syk-dependent actin organization governs FcγR mobility.

- Actin reorganization during phagocytosis regulates FcγR mobility and clustering.
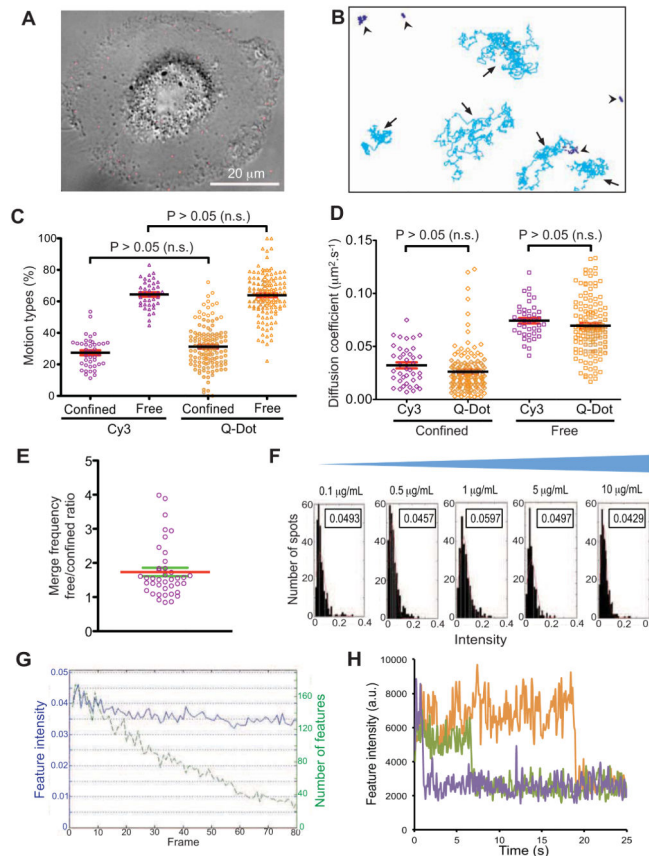
Figure 1. Single-molecule imaging of FcγRIIA reveals heterogeneous mobility in human primary macrophages

A. Low density labelling of FcγRIIA with Q-dots (red) at the surface of primary monocyte-derived macrophages. Representative image of more than 100 cells, from more than 10 independent experiments.

B. Tracks obtained by SPT of FcγRIIA in one representative field of view. Confined motion is represented in navy blue and pointed by arrowheads; free motion is represented in cyan and pointed by arrows. Representative field of more than 100 cells, from more than 10 independent experiments.

C. Percentage of confined receptors (circles) and free receptors (triangles), labelled with Cy3 (purple) or Q-dot (orange). Each dot represents one individual cell. Mean (black bar) and standard error to the mean (red bars) are displayed for each population. 18756 tracks from n = 40 cells and 27506 tracks from n = 130 cells were analysed for Cy3 and Q-dot labelled cells, respectively.

D. Median diffusion coefficients of confined receptors (diamonds) and free receptors (squares), labelled with Cy3 (purple) or Q-dot (orange).

E. Ratio of merge frequency between free receptors and confined receptors, labelled with Cy3. Each dot represents one individual cell. 18756 tracks from n = 40 cells were analysed.

F. Fluorescence intensity histograms of detected Cy3-labelled FcγRIIA with different primary Fab concentrations (in μg/mL) in fixed cells. Intensity modes were analysed with a Gaussian fit (red line) and their mean intensity value is reported in the top right boxes.

G. Average fluorescence intensity of detected particles determined by Gaussian fitting (blue), and number of detected particles (green), measured over time during photobleaching experiments with Cy3-labelled FcγRIIA in fixed cells.

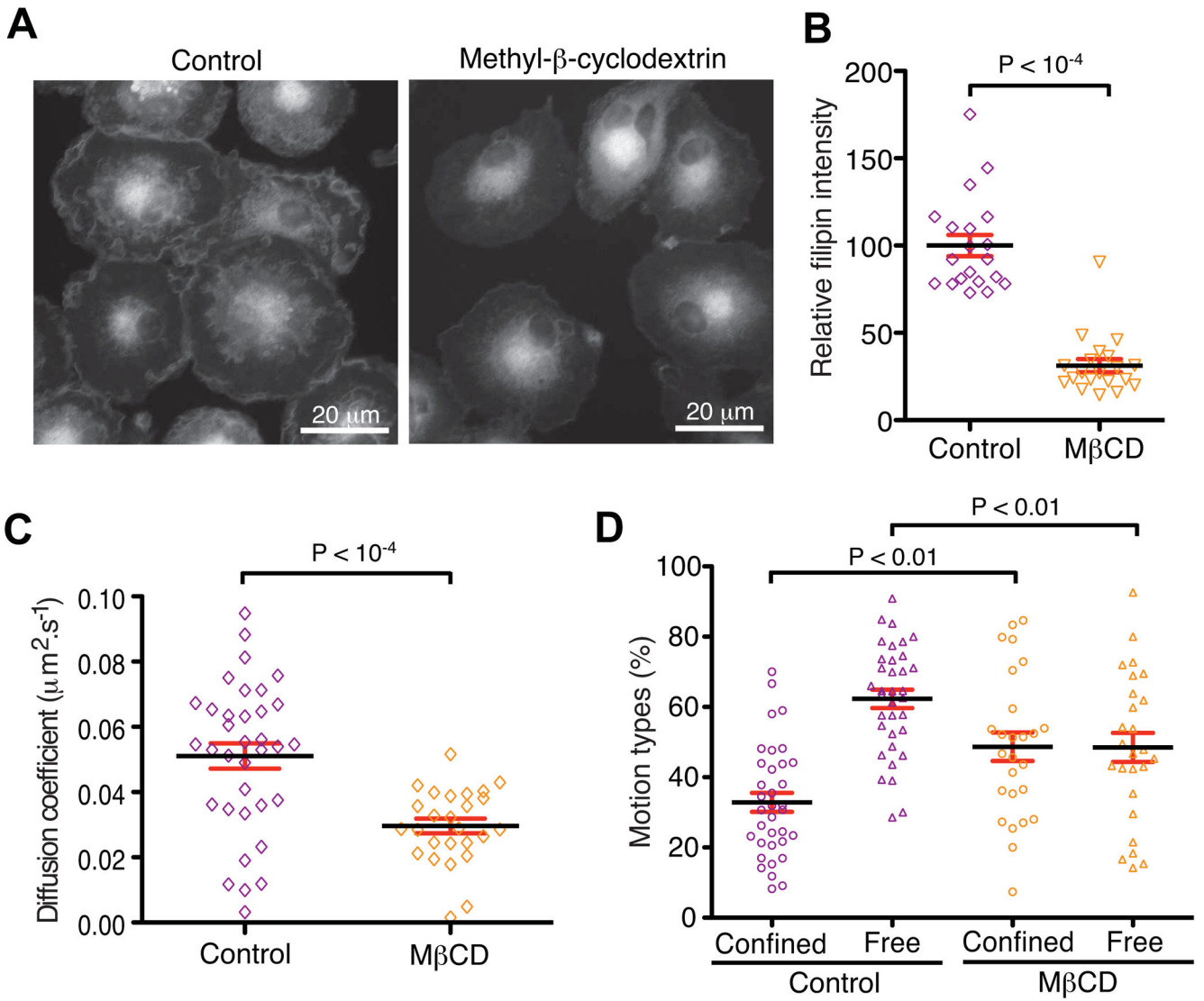H. Representative measurements of the fluorescence intensity of individual features over time, illustrating photobleaching events.

Figure 2. FcγRIIA mobility is not confined by cholesterol-rich microdomains

A. Filipin staining of cholesterol in primary human macrophages. Representative images of more than 30 fields, from 3 independent experiments.

B. Quantification of filipin intensity at the plasma membrane on individual primary macrophages. Measurements of each separated experiment were normalized to the mean intensity of the control cells.

C. Median diffusion coefficient (for all particles regardless of motion type) in control (purple) and methyl-β-cyclodextrin treated cells (orange). 8790 tracks from 35 cells and 5640 tracks from 26 cells were analysed for control and methyl-β-cyclodextrin-treated cells, respectively.

D. Percentage of confined receptors (circles) and free receptors (triangles), in control (purple) and methyl-β-cyclodextrin treated cells (orange).
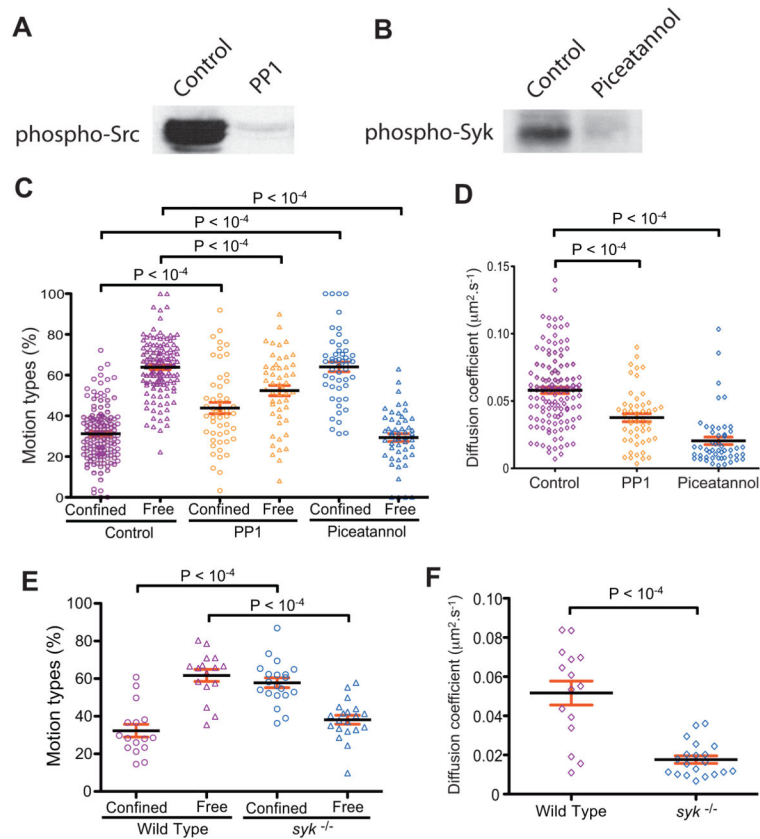
Figure 3. FcγRIIA mobility is regulated by Syk and Src-family kinases

A. Endogenous Src activity revealed by anti-phospho-Src Y416 immunoblotting in resting untreated or PP1 treated primary human macrophages. Representative western blot from 3 independent experiments.

B. Endogenous Syk activity revealed by anti-phospho-Syk Y525/526 immunoblotting in resting untreated or piceatannol treated primary human macrophages. Representative western blot from 3 independent experiments.

C. Percentage of confined FcγRIIA (circles) and free FcγRIIA (triangles), in control (purple), PP1 (orange) and piceatannol-treated (blue) primary human macrophages. 27506 tracks from n = 130 cells, 7768 tracks from n = 50 cells and 7027 tracks from n = 51 cells were analysed for control, PP1 and piceatannol treated cells, respectively.

D. Median diffusion coefficients of FcγRIIA in control (purple), PP1 (orange) and piceatannol (blue) treated primary human macrophages.

E. Percentage of confined FcγR (circle) and free FcγR (triangle), in wild type (purple) and $syk^{-/-}$ (blue) mouse bone marrow-derived macrophages. 9747 tracks from n = 16 cells and 18955 tracks from n = 20 cells were analysed for wild type and $syk^{-/-}$ macrophages, respectively.

F. Median diffusion coefficients of FcγR in wild type (purple) and $syk^{-/-}$ (blue) mouse bone marrow-derived macrophages.
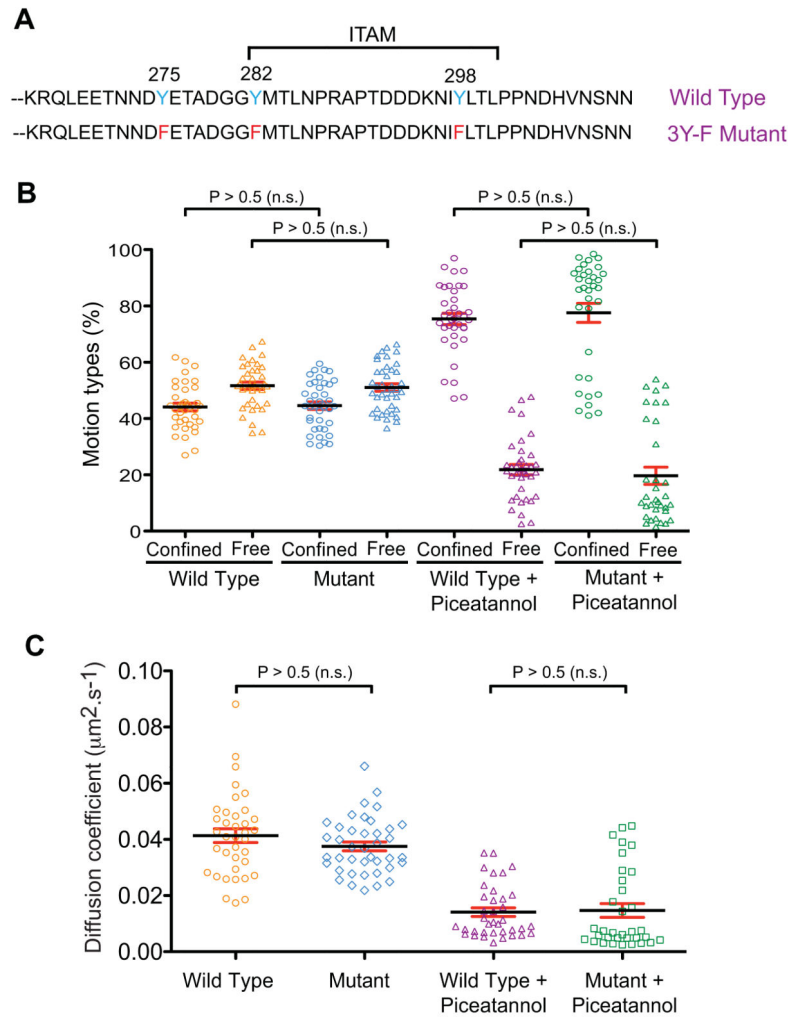
Figure 4. Receptor tyrosine phosphorylation does not account for FcγRIIA confinement in resting macrophages

A. Amino acid sequence of FcγRIIA cytosolic tail. The three tyrosines (blue) in the wild type protein were replaced by phenylalanines (red) in the 3Y-F mutant construct.

B. Percentage of confined receptors (circles) and free receptors (triangles), observed for wild type or 3Y-F mutant receptors in control (orange and blue, respectively), or piceatannol treated (purple and green, respectively) RAW 264.7 macrophages. 24367 tracks from n = 37 cells, 41272 tracks from n = 40 cells, 11184 tracks from n = 37 cells and 15053 tracks from n = 34 cells were analysed for wild type, wild type + piceatannol, mutant and mutant + piceatannol cells, respectively.

C. Median diffusion coefficients observed for wild type or 3Y-F mutant receptors in control (orange and blue, respectively), or piceatannol-treated (purple and green, respectively) RAW 264.7 macrophages.
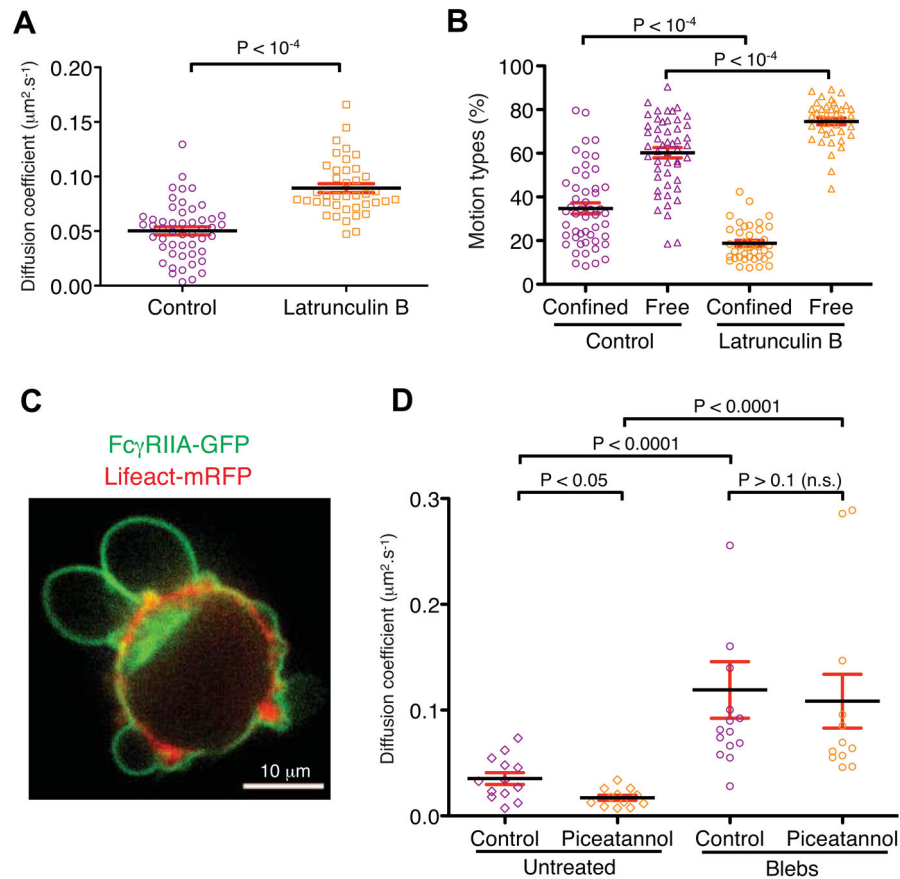
Figure 5. FcγRIIA mobility is restricted by the actin cytoskeleton

A. Median diffusion coefficient in control (purple) and latrunculin B-treated human primary macrophages (orange). 6005 tracks from n = 50 cells and 5959 tracks from n = 40 cells were analysed for control and latrunculin-treated cells, respectively.

B. Percentage of confined receptors (circles) and free receptors (triangles), in control (purple) and latrunculin B-treated cells (orange).

C. Confocal image of bleb formation in RAW 264.7 macrophages upon jasplakinolide treatment; FcγRIIA-GFP (green) and LifeAct-mRFP (red). Representative image of more than 20 cells from 3 independent experiments.

D. Diffusion of FcγRIIA-GFP determined by FRAP at the plasma membrane of untreated RAW macrophages (diamonds) or in the blebs of jasplakinolide treated RAW macrophages (circles), in presence (orange) or absence (purple) of piceatannol.
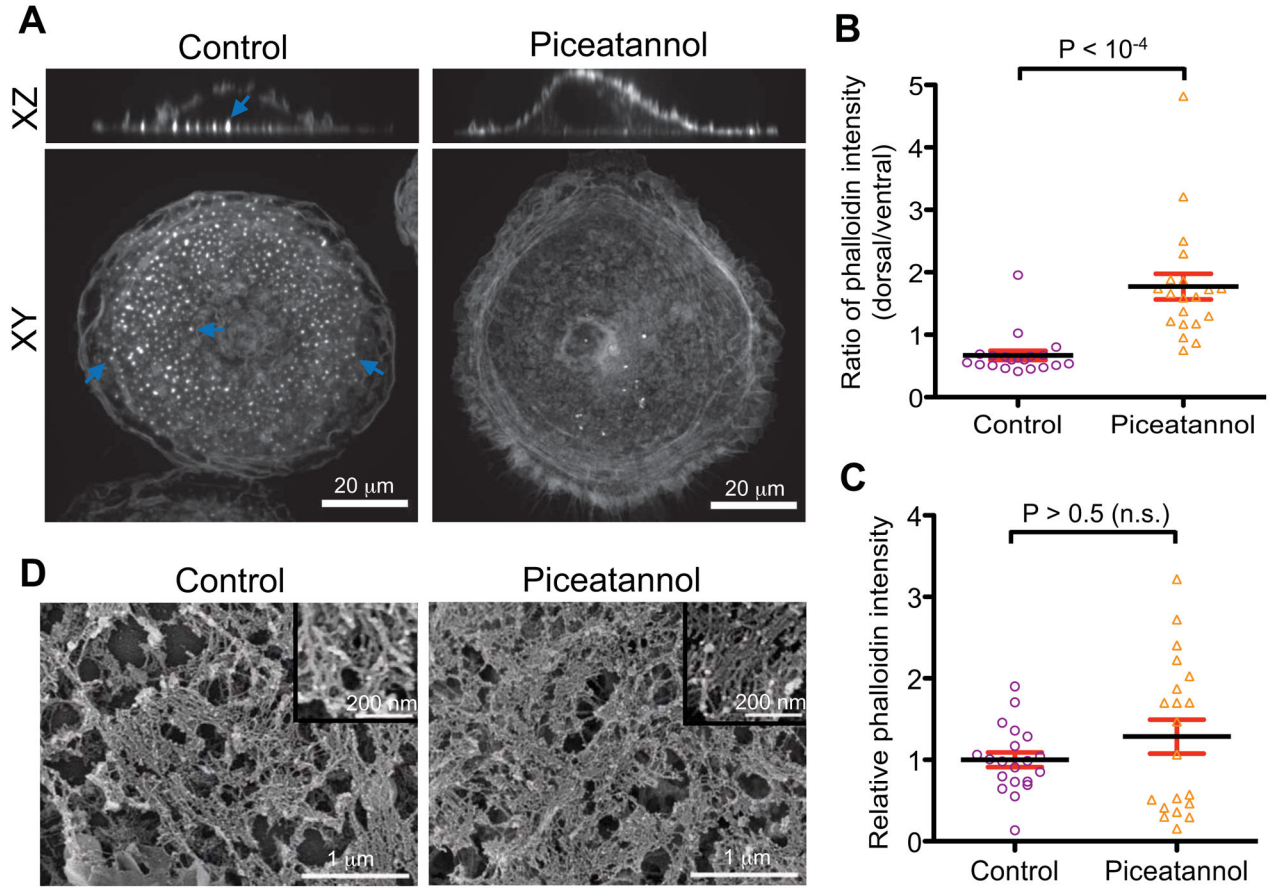
Figure 6. Syk inhibition leads to a large redistribution of the actin cytoskeleton in human primary macrophages

A. Confocal images of phalloidin-labelled F-actin distribution in human primary macrophages. Top panel: transversal slice, bottom panel: Z projection of maximal intensities. Representative images of more than 50 cells from more than 10 independent experiments. Blue arrows indicate podosomes.

B. Ratio of phalloidin intensity between the dorsal and ventral surface of individual cells. Measurements of each separated experiment were normalized by the mean intensity of the control cells.

C. Quantification of total phalloidin intensity on individual cells. Measurements of each separated experiment were normalized by the mean intensity of the control cells.

D. High resolution scanning electron microscopy of the cortical cytoskeleton of human primary macrophages after detergent-based plasma membrane removal. Representative images of at least 12 cells from 3 independent experiments.
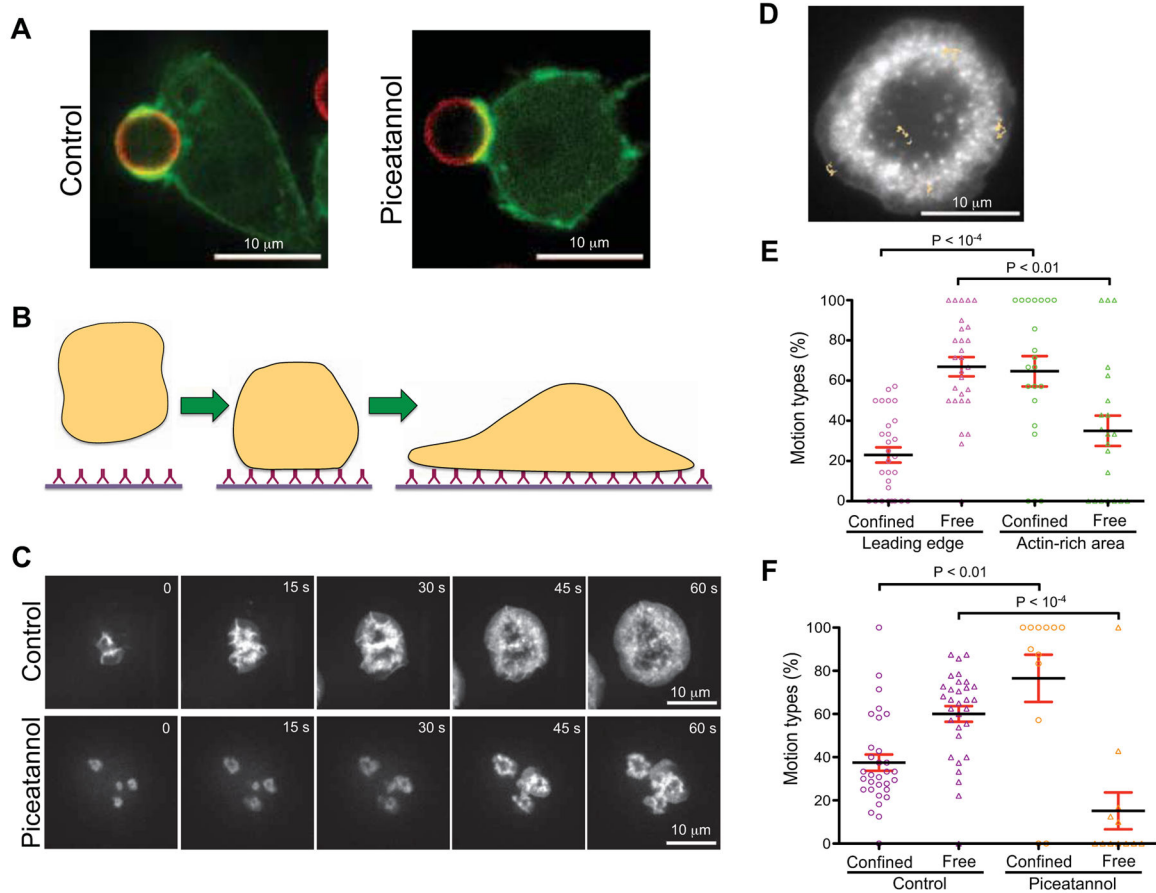
Figure 7. Syk-mediated actin reorganization of the actin cytoskeleton dictates FcγR mobility during phagocytosis

A. Confocal images of F-actin localization Fc-mediated during phagocytosis in RAW 264.7 macrophages in absence (left) or presence (right) of piceatannol. LifeAct-GFP (green), IgG-coated 5 μm polystyrene beads (red). Representative image of at least 12 cells from 3 independent experiments.

B. Schematic of the frustrated phagocytosis model on IgG-coated coverslips.

C. Time series of confocal images of actin-GFP distribution during frustrated phagocytosis, at the surface in contact with the coverslip, in untreated (top panel) or piceatannol treated (bottom panel) RAW macrophages. Representative images of more than 30 cells from 5 independent experiments.

D. FcγR mobility within the phagocytic cup in RAW 264.7 macrophages. Tracks obtained by SPT of Fcγ during 5 sec (beige) are overplayed on the image of Actin-GFP (grey). Representative image of more than 50 cells from more than 5 independent experiments.

E. Percentage of confined receptors (circles) and free receptors (triangles), observed in the actin-poor leading edge (pink) of the actin-rich area (green) during frustrated phagocytosis. 398 tracks from n = 27 cells were analysed.

F. Percentage of confined receptors (circles) and free receptors (triangles), observed during frustrated phagocytosis in untreated (purple) or piceatannol treated (orange) RAW

macrophages. 11 tracks from n = 11 cells and 55 tracks from n = 15 cells were analysed for control and piceatannol-treated cells, respectively.